Addis Ababa University

Addis Ababa Institute of Technology (AAiT)

School of Electrical and Computer Engineering

Communication Engineering Graduate Program

Real-time Feature Extraction in a Distributed Acoustic Sensor Based on Phase Demodulation With Fast Hilbert Transform

by

Semira Mohammed

Advisors: Dr. Yonas Seifu

Dr. Bisrat Derebssa

A Thesis Submitted to the School of Graduate Studies of Addis Ababa University in Partial Fulfillment of the Requirement for the Degree of Master's Science in Communication Engineering

March 2024

Addis Ababa, Ethiopia

Adis Ababa University
Addis Ababa Institute of Technology
School of Electrical and Computer Engineering
Communication Engineering Graduate Program

Real-time Feature Extraction in a Distributed Acoustic Sensor Based on Phase Demodulation With Fast Hilbert Transform

by:

Semira Mohammed

Approval by Board of Examiners	Signature	Date
Chairman, School Graduate Comittee:	_____	_____
Dr. Bisrat:	_____	_____
Internal Examiner's Name:	_____	_____
External Examiner's Name:	_____	_____

Declaration

I, declare that this thesis "Real-time Feature Extraction In A Distributed Acoustic Sensor Based On Phase Demodulation With Fast Hilbert Transform" is my own work, that it has not been submitted before for any degree or assessment at any other university, and that all the sources I have used or quoted have been indicated and acknowledged by means of complete references.

Name of the Student	Signature	Date
_____	_____	_____

This thesis has been submitted for examination with my approval as a university advisor.

Name of the Advisor	Signature	Date
_____	_____	_____

Addia Ababa, Ethiopia

Abstract

Phase-sensitive optical Time Domain Reflectometry (Φ-OTDR) is the most common implementation of a Distributed Acoustic Sensor (DAS) system. It employs the observation of speckles resulting from Rayleigh Back-scattering from coherent pulses in an optical fiber[1]. Since they are sensitive to local disturbances altering the intensity and phase of light, perturbations induced by events cause changes in the speckle pattern whose precise measurement provides information on the amplitude and frequency of vibrations distributed along the fiber. Demodulation of the local phase change is key to the precise measurement of events since it is more linearly related to the strain applied to the fiber. One of the key issues in distributed sensing is that phase demodulation schemes usually require additional post-processing algorithm runs for each spatial location, which introduces delays, and hence reductions in dynamic sensing capability when scaled along the whole sensing distance.

In this research, we analyze the impact of the post-processing in different phase demodulation techniques employing Phase-Generated Carrier (PGC) on the bandwidth of distributed feature extraction in a typical DAS system by quantifying the total computation time needed for a benchmark, 10-km sensing range at meter-scale and sub-meter-scale spatial resolutions. We then design, implement, and analyze a signal processing scheme for phase extraction in Φ -OTDR enabling real-time dynamic measurements based on a Fast Hilbert Transform (FHT). Particular focus is given to the choice of this demodulation scheme for optimizing the bandwidth of distributed feature extraction as it enables the use of parallel processing of adjacent blocks in such a way that the overall throughput of spatially resolved concurrent demodulation allows dynamic vibration sensing at speeds relevant to most distributed monitoring applications. Our analysis shows that that on average 3 orders magnitude reductions in computation times are achieved when employing the Fast Hilbert transform for demodulation compared to the commonly used PGC-arctan algorithm, while there is a three-fold reduction compared to PG-DCM and PG-DMS algorithms.

Keywords

Phase-Sensitive Optical Time Domain Reflectometry (Φ-OTDR), Phase-Generated Carried Demodulation, Fast Hilbert Transform (FHT), and Distributed Acoustic Sensing (DAS).

Acknowledgements

I would like to express my sincere gratitude to all those who have contributed to the completion of this MSc thesis.This academic journey has been both challenging and rewarding, and I am deeply thankful for the support and guidance I have received along the way. First and foremost, I am grateful to my thesis advisors, Dr.Yonas Seifu and Dr.Bisrat Derebssa, for their invaluable guidance, insightful feedback, and unwavering support throughout the entire research process. Their expertise and encouragement have been instrumental in shaping the direction of this study. I would like to acknowledge the assistance and cooperation of my fellow classmates and colleagues. Their camaraderie and shared experiences have created a positive and motivating atmosphere, contributing significantly to the success of this endeavor.I am also indebted to Addis Ababa University for its financial support, which enabled me to dedicate time and resources to this research project. Finally, I offer special thanks go to my family for their unwavering support, understanding, and encouragement. Their belief in my abilities has been a constant source of motivation, and I am grateful for their love and encouragement.

Contents

List of Figures

Abbreviations

DAS	**D**istrubuted **A**coustic **S**ensor
Φ-OTDR	**P**hase-sensitive **O**ptical **T**ime **D**omain **R**eflectometer
LabVIEW	**L**aboratory **V**irtual **I**nstrument **E**ngineering **W**orkbench
SNR	**S**ignal-to- **N**oise **R**atio
RTT	**R**ound-**T**rip **T**ime
DAQ	**D**ata **AQ**uisition system
EDFA	**E**rbium **D**oped **F**iber **A**mplifier
WDM	**W**avelength **D**ivision **M**ultiplexing
FHT	**F**ast **H**ilbert **T**ransform
PGC-DCM	**P**hase **G**enerated **C**arrier- **D**ifferential-**C**ross- **M**ultiplying
PGC-DMS	**P**hase **G**enerated **C**arrier **D**ifferentiate**M**ultiply and **S**quare
FBG	**F**ibre **B**ragg **G**rating
PZT	**P**iezoelectric **T**ransducers
UWFBG	**U**ltra- **W**eak **F**ibre **B**ragg **G**rating
PGC	**P**hase **G**enerated **C**arrier
LID	**L**ight **I**ntensity **D**isturbance
MHZ	**M**ega **H**ertz
PD	**P**hoto **D**etector
FOIS	**F**iber- **O**ptic **I**nterferometric **S**ensor
LPF	**L**ow **P**ass **F**ilter
UV	**U**ltra **V**iolet
CMOS	**C**omplementary **M**etal- **O**xide- **S**emiconductor
MZI	**M**ach- **Z**ehnder **I**nterferometer
NI	**N**ational **I**nstruments
VI	**V**irtual **I**nstruments

Chapter 1

Introduction

1.1 Background

1.1.1 Fiber Optics

The history of fiber optics is a tale of scientific curiosity turned technological revolution. In the 19th century, John Tyndall laid the theoretical groundwork by demonstrating the principle of total internal reflection, essential for guiding light through transparent materials. However, it was not until the 1950s and 1960s that researchers like Harold Hopkins and Narinder Kapany began making practical strides. Kapany, often hailed as the "father of fiber optics," significantly contributed to light transmission through glass fibers. The 1966 proposal by Charles Kao and George Hockham marked a turning point, leading to Kao's later Nobel Prize for his work. By the 1970s and 1980s, commercialization took flight with Corning's low-loss optical fibers, setting the stage for long-distance, high-capacity communication. Technological advances, such as wavelength-division multiplexing (WDM) and erbium-doped fiber amplifiers (EDFAs), further enhanced the span and bandwidth of optical communication . Today, fiber optics are the linchpin of modern telecommunications, driving high-speed internet, telephone systems and cable television, with ongoing research continuing to expand the capabilities of this transforming technology.[2]

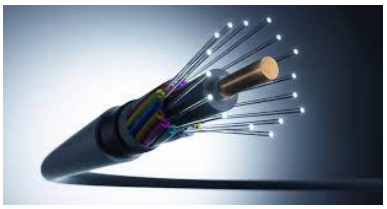

FIGURE 1.1: fiber optic cable[2].

1.1.2 Distributed Acoustic Sensing(DAS)

Distributed Acoustic Sensing (DAS) is a revolutionary technology that transforms standard optical fibers into multiple, extraordinarily sensitive and versatile sensors. Unlike traditional point or static sensors, DAS allows for continuous, real-time monitoring of acoustic signals along the entire length of the optical fiber. This capability is achieved by exploiting the phenomenon of coherent Rayleigh scattering, where imperfections in the fiber cause scattered light that can be analyzed to detect acoustic disturbances.[7]

In a DAS system, light is sent into an optical fiber, and as it propagates to the far end, a tiny fraction of the light is backscattered to the near end. The backscattred light's intensity changes When minute variations are induced at any location in the fiber by external impacts, such as sound waves or vibrations. These disturbances effectively modulate the properties of the scattered light, and by precisely analyzing the intensity and phase of the backscattered light, DAS can convert the optical fiber into a distributed sensor capable of detecting and locating acoustic events with impressive precision.[8] It finds utility in monitoring pipelines for leaks or intrusions, securing perimeters by detecting footsteps or vehicle movements, and even in seismic sensing for early earthquake detection. The ability to repurpose existing optical fiber infrastructure for sensing purposes makes DAS a cost-effective and scalable solution for various industries, ranging from oil and gas to transportation and security. As technology continues to advance, DAS holds the potential to redefine how we perceive and respond to acoustic events across vast and complex environments.[6] DAS based on Phase-sensitive Optical Time-Domain Reflectometry (Φ-OTDR) is a ubiquitous sensing scheme offering innovative solutions for monitoring and securing critical infrastructure. These technologies harness the unique properties of optical fibers to convert them into sensitive and versatile sensors, enabling real-time, continuous monitoring of physical parameters along the entire length of the fiber and is suitable for applications such as pipeline and perimeter security, as well as seismic monitoring. DAS based on Φ-OTDR utilizes

the change in phase information of the backscattered light to detect disturbances and events with high spatial resolution, making it ideal for applications such as dynamic strain sensing in structural health monitoring and intrusion detection [9]. Fiber optic sensing for distributed dynamic monitoring has recently received a lot of attention, owing to the many applications it provides in real-time safet and integrity monitoring and DAS constitutes a key component of such systems. According to a recent analysis, DAS's worldwide market share is rising gradually and is expected to generate more than 2 billion in sales by 2025.[10] The approach has a number of potential uses in a variety of industrial domains, such as the integrity and safety monitoring of big buildings, oil-gas pipelines, and railway systems. A popular sensing method for DAS, phase-sensitive optical time domain reflectometry (Φ-OTDR) is based on the detection of phase-sensitive coherent Rayleigh speckles in the time domain. This approach produces coherent Rayleigh backscattering that exhibits a dispersed speckle pattern that is sensitive to local phase shifts brought on by external impacts. The coherent light source pulses are transmitted into a sensor fiber.[6] A change in the optical fiber is caused by a local disturbance. The theoretical upper limit on the frequency of impact The round-trip time (RTT) of light along the path determines the signal that can be extracted. Because of the fiber, the technique is suitable for high-frequency vibration measurements. Several techniques for extracting perturbations in Φ-OTDR have been proposed, most notable of them concentrating on measuring the location, amplitude, and frequency of the received signal, on which part of the disturbance information can be encoded. The use of a straightforward direct detection scheme for intrusion detection and a differential intensity trace for impact extraction are examples of early implementations. There have also been other proposed schemes that involve the resolution of the backscattered signal in the wavelet domain. In more modern schemes, the signal-to-noise ratio of the backscattering signal is enhanced in the vibration measurement through advanced signal processing[11].

1.2 Statement of the problem

Analyzing the evolution of the received signal across different spatial locations provides valuable insights into the distributed impact under observation. However, a significant impediment to the progress of Distributed Acoustic Sensing (DAS) lies in the challenge of implementing cost-effective interrogation schemes for dynamic measurements. One of the key issues in distributed sensing is that phase demodulation schemes usually require additional post-processing algorithm

runs for each spatial location, which introduces delays, and hence reductions in dynamic sensing capability when scaled along the whole sensing distance. Measurement of the phase in a distributed scheme poses issues of latency, especially in applications whereреal-time monitoring is necessary. Overcoming this challenge is crucial for practical realization and scalable commercialization of DAS. This involves careful consideration of the specific signal processing methods employed to capture phase changes resulting from external impacts. [12][13] The frequency of the impact signal that can be reliably extracted is theoretically limited by the round-trip time (RTT) of light along the fiber. DAS addresses these limitations as is particularly adept at high-frequency vibration measurements over extended distances. In addressing these challenges, we propose an innovative approach for DAS, analyzing the performance of phase demodulation techniques and identifying the robust algorithms with more suitability to dynamic distributed sensing applications. The choice of the algorithm must also be informed by recent advances in signal processing techniques and tools, which are keys to improving the speed and efficienty of vibration measurements over long distances and simplifying the overall sensing system.

1.3 Objectives of the Research

1.3.1 General Objective

The general objective of this thesis is to analyze some representative phase demodulation techniques and improve the signal processing scheme for real-time feature extraction in a distributed acoustic sensor based on phase demodulation with a Fast Hilbert Transform.

1.3.2 Specific Objectives

This thesis specifically aims to achieve the following specific objectives:

- Comprehensive study of different demodulation of Phase-sensitive Optical Time Domain Reflectometry (Φ-OTDR), schemes, and fast Hilbert transform.
- Comparisons of different demodulation techniques by simulation using MATLAB and LabVIEW software.
- Implementation of the proposed signal processing scheme for a DAS based on (Φ-OTDR) using FHT for demodulation DAS over a representative distance of 10 km on a standard single-mode fiber.
- Comparison of the dynamic performance of the proposed method against other commonly used demodulation schemes

1.4 Methodology

To achieve the aforementioned objectives the following methods will be used:

- Literature review: includes reading books, journals, and related work and other relevant about DAS, different demodulation of Phase-sensitive Optical Time Domain Reflectometry (Φ-OTDR) schemes, and fast Hilbert transform, and how to improve optical signal processing.
- Data collection and analysis: involves reviewing the mechanism of phase demodulation in delayed interferometric sensor and presenting the mathematical background of the demodulation techniques used in a Distributed Acoustic Sensor. It also includes calculating the relative time difference.
- Simulation and interpretation of the result: involves the simulation of different demodulation algorithms in Phase-sensitive Optical Time Domain Reflectometry (Φ-OTDR) scheme (including PGC-DCM, PGC-DMS, PGC-arctan). Then, the results will be compared to each other and with FHT-based demodulation algorithm.

- Documentation: Finally, we will prepare the documentation reporting the detailed implementation and computing the performance metrics for multiple distributed sensing scenarios.

  It will also involve the performance comparison demodulation of Phase-sensitive Optical Time Domain Reflectometry (Φ-OTDR).

1.5 Motivation

Distributed acoustic sensing (DAS) is a technology that enables continuous real-time measurement of vibrations along an entire length of an optical fiber. While the frequency and position of disturbances can be retrieved from intensity measurements, phase extraction with various demodulation techniques offers more accurate quantitative measurements. Phase-sensitive optical time-domain reflectometry (Φ-OTDR) is widely used in DAS. On the other hand, the Fast Hilbert Transform (FHT) is useful for computing instantaneous properties of time series, especially amplitude and frequency. This is a simple and convenient algorithm for instantaneous frequency extraction of a signal, and FHT has clear benefits when applied in long distance sensing with thousands of sensing points, also owing to efficient implementation of the computation in the algorithm.

1.6 Scope of the research

This thesis addresses the advantages of using an advanced signal processing scheme for real-time feature extraction in a distributed acoustic sensor based on phase demodulation with FHT. It gives an insight into the performances of different demodulation techniques when used in a representative DAS system. Through investigations pivoting on overall processing times in distribued sensing, the study aims to contribute to the advancement of demodulation techniques in DAS applications. The findings of this research will provide valuable insights into the suitability and wide variance in the performance of different demodulation techniques, thereby enabling sensing system developers to make informed decisions when choosing the most appropriate approach for phase demodulation in real-time measurements in DAS.

1.7 Contributions of the Research

In this thesis, we analyze representative phase demodulation algorithms used in a DAS based on Φ-OTDR sensor in a direct detection and pulse probe for distributed dynamic phase change extraction employing a reliable interferometric demodulation method that is ideal for distributed dynamic sensing. We utilize the single point fast Hilbert transform and contrast the performance with commonly used phase demodulation methods. Next, we design signal processing schemes for a representative physical setup used to implement the proposed sensing scheme and quantify the relative impact of phase demodulation in the overall processing time for varying sensing distances and offer comparisons of the various algorithms' computation time responses.

1.8 Research Layout

Chapter 1: Introduction - this chapter provides an introduction to the thesis, outlining the problem statement, objectives, methodology and motivation of real time extraction in DAS employing phase demodulation with FHT.

Chapter 2: Literature Reviews - a comprehensive review of the literature and an overview of some of the recent advances of research in the area of DAS based on (Φ-OTDR).

Chapter 3: Analysis and design - detailed implementation, analysis and design of signal processing schemes for phase extraction in Φ-OTDR enabling real-time dynamic measurements based on a Fast Hilbert Transform (FHT).

Chapter 4: Results and Discussion - this chapter presents and compares simulation results obtained from the implementation in LabVIEW.

Chapter 5: Conclusion and Future work - the final chapter serves as a conclusion to the thesis, summarizing key findings and presenting suggestions for future investigation in demodulation schemes for DAS.

Chapter 2

Literature Review

Phase-sensitive optical time domain reflectometry has already been the subject of several contributions and investigations. In order to gather only a portion of the information about the disturbance, such as its exact location and frequency, early Φ-OTDR implementations concentrated on measuring the change in intensity and frequency of the backscattering signal from each location along the sensing fiber. The following, among other things, are once again examined to align the current study with the issue at hand.

Authors in [3] report on a scheme which enhances the signal's SNR, including the use of advanced signal processing with optical pulse coding for fast denoising. The method involves sending multiple pulses in the sensing fiber instead of a single one and obtaining the single pulse equivalent via decoding. Instead of using a single pulse in the sensing fiber, the method sends multiple pulses, which are then decoded to produce the equivalent single pulse. With this technique, low-cost DFB lasers with linewidths in the order of a few MHz can be used to measure distributed vibration more accurately. This is made possible by adding two coherence conditions that specify the bit time—the interval of time between successive pulses—and the range of the line width of the light source that is used. These are the inter-pulse incoherence condition, which demands that there be no coherence between signals in consecutive pulses to prevent interference from the backscattering from adjacent pulses, and the intra-pulse coherence condition, which demands that there be coherence within the pulse width.

within Φ-OTDR systems[12]. A High-SNR DAS has also been implemented using mulitiple ultra-weak gratings which induce higher backscattering. Authors in [13] used an array of identical UWFBG (Ultra- Weak Fibre Bragg Grating)

gratings as transducers, using a delay interferometry technique showing phase demodulation in one arm and delay in the other arm, and along with a scalable demodulation, demonstrate high SNR DAS based on Φ- OTDR. As opposed to writing multiple FBGs, this system's less complicated fabrication process is based on the cost-effective technique of UV light-exposing a single-mode fiber without the need for key alignment. The method employs a scheme based on PGC demodulation using the Differentiate and Cross Multiply (PGC-DCM) algorithm. The scheme presented in is suitable for distributed sensing as the mechanism for the phase interrogation uses a single narrow band receiver with direct detection by a single-pin photo diode, while automatically avoiding the computationally intensive phase unwrapping algorithm in PGC-arctan demodulation. A tenfold increase in the detected backscattering amplitude from the ultra-weak gratings is the reason why the method produces improved signal-to-noise ratio.

Additionally, PGC-DCM does not require complex phase deconvolution algorithms, making it suitable for distributed measurements. Further research also shows that PGC-DCM is robust against unwanted harmonic distortions. Harmonic distortion is high using the PGC-arctan method when the modulation depth deviates from the nominal value [4]. Since there is no division operation, the PGC-DCM method is also suitable for situations where one of the intermediate signals used to obtain the demodulation phase has multiple zero-crossing points, avoiding additional mechanisms to reduce the division-by-zero operation can.

Another interesting feature of PGC-DCM algorithm is that it also includes symmetric derivative and integral operations that are particularly suited for analog processing systems. Mainly thanks to the rich techniques of fractional order calculus [14].
Most recent implementations of phase demodulation methods [15] do not rely on coherent detection. It has been effectively demonstrated for probes with a single pulse as well as those with two pulses. Using this method, phase information is retrieved by recording two backscattering intensity signals that are generated at a particular point in the fiber during a disturbance. By analyzing the delayed interference of backscatterign between adjancent points, the phase can be accurately determined without the need for coherent detection. Such a method offers advantages such as simplicity and cost-effectiveness compared to techniques that require coherent detection. It's important to note that further research is still being conducted to explore the full potential and limitations of this technique. However,

preliminary results show promising outcomes in terms of phase demodulation accuracy and feasibility. Another approach for phase extraction involves the use of coherent homodyne detection, as described in reference [16]. In this method, the backscattering signal is combined with a local oscillator and fed into a 90° hybrid. This allows for the extraction of the two orthogonal components of the signal which are used to obtain the phase with the arctan and subsequent phase unwrapping. The study reported in reference [44] demonstrates the effectiveness of this method by achieving demodulation of a 600 Hz signal over a distance of 12.56 km, with a resolution of 10 m. By employing coherent homodyne detection with a 90° hybrid and a local oscillator, the researchers were able to accurately extract the phase information from the backscattered signal. This technique has shown promising results and has the potential to enhance the performance of phase demodulation in distributed acoustic sensing systems. It is worth mentioning that other distributed strain measurements are inherently static. For instance Brillouin Optical Time-Domain Analysis (BOTDA) involves the use of stimulated Brillouin scattering, whose spectrum is dependent on strain and temperature. A recent study in[17] involved a field static load test where the variation of strain along a precast pile was measured using the differential pulse-pair BOTDA (DPP-BOTDA) interrogator. Once the RANSAC processed strain data was obtained, the axial force and frictional resistance were then calculated, allowing for the estimation of pile-soil interface properties. The results demonstrated the feasibility and good performance of DPP-BOTDA in measuring precast piles' stress.

Additionally, the effectiveness of the RANSAC method in processing DFOS data with a certain number of outliers was also evident. This scheme's performance has been enhanced in a study [5] with respect to both spatial and frequency resolutions. In the revised setup, the Amplified Spontaneous Emission (ASE) noise in the backscattering signal and the propagating pulses is filtered using a single Fiber Bragg Grating (FBG). When compared to using two separate FBGs, this method is more efficient because it allows for the narrow design of a single FBG without the need to match the central wavelength. This technique has achieved a frequency resolution that can be lowered to 5 Hz and has been successfully used to measure dynamic perturbations up to 3 kHz at a distance of 5 kilometers.

In addition, this scheme for phase unwrapping uses a fringe counting algorithm, which does add extra post processing overhead. This overhead takes on a multi-dimensional nature in a distributed scenario encompassing several points. Moreover, the interferometer must be thermally isolated for the receiver of this scheme to function, and three separate photodiodes must be used and operated synchronously. As a result, in comparison to other options, the receiver of this scheme

is somewhat more complex.

The aforementioned papers highlight the significance phase demodulation in Φ-OTDR. However, so far, the computation times for phase demodulation algorithms including fast Hilbert transform in distributed sensing systems have not been properly quantified. Therefore, this thesis aims to explore algorithms used for phase demodulation in distributed acoustic sensing in terms of their dynamic performances and seeks to examine the benefits of demodulation with fast Hilbert transform.

The fast Hilbert transform is a mathematical tool used for fast computations of the analytic signal associated with a real-valued input signal, which in turn enables fast extraction of phase information from the backscattered signals, making it suitable for real-time monitoring of dynamic events over a long sensing span.

The aim of this research is to make a quantitative comparison of computation times of conventional demodulation schemes in DAD with one based on FHT. The algorithms will be carefully designed and implemented to ensure a fair comparison of their suitability for efficient phase demodulation. By quantifying the processing times of phase demodulation algorithms for distributed acoustic sensing using fast Hilbert transform, this thesis aims to contribute to the advancement of efficent Φ-OTDR schemes and their applications in various areas such as structural health monitoring, perimeter security as well as and oil and gas pipeline monitoring.

Chapter 3

Theory and Analysis

The widely used method for putting Distributed Acoustic Sensing systems into practice is the Φ-OTDR scheme, which depends on coherent Rayleigh backscattering from a time-domain sensing fiber. The sensing fiber is modeled as a collection of M random scattering elements, each with a reflectivity of $ri \ll 1$, according to the operational concept of Φ-OTDR. These elements backscatter coherent pulse light that reaches them, and because of light coherence, the field contributions from nearby elements within the pulse's spatial length show comparable phase relations. This causes interference at the receiver, which is highly sensitive to nearby disturbances and results in a distributed coherent speckle pattern. Therefore, this scheme is appropriate for distributed dynamic monitoring systems for multiple real-time vibration measurements and can be used to measure vibrations at a high repetition rates.

3.1 Phase generated carrier (PGC)

Phase-generated carrier (PGC) demodulation is widely used in optical fiber interferometers due to its high sensitivity, large dynamic range, and high signal fidelity. The proposed algorithm provides real-time compensation for carrier phase delay and modulation depth without additional compensates. Phase changes can be quantified dynamically from a single disturbance point along an optical fiber using interferometric techniques [18, 19].

Concurrent demodulation of phase changes from multiple impact points using interferometric configurations requires additional complex setups[20, 21].By first sending two adjacent pulses into the sensing fiber and then using the interaction

between the backscattering from the two pulses, it is possible to perform a similar demodulation in Φ-OTDR using a double pulse probe[22].The fundamental schematic of the particular double pulse method shown in the figure 3.1, which displays the backscattering signal from two nearby locations crossed by the double pulse indicated along the fiber with locations m and k justΔz away from one another, where one pulse is phase-modulated selectively with$\Delta\delta(t)$. When an outside disturbance applying the phase change $\Phi(t)$ to the area between these two points, There is an electric field in the backscattering at the receiver from each position,$E_{m,k}\,(t)$. provided by:

$$\begin{aligned} E_m(t) &= E_m \exp[j\delta_m(t) + j\phi_m], \\ E_k(t) &= E_k \exp[j\phi(t) + j\delta_k(t) + j\phi_k], [10] \end{aligned} \tag{3.1}$$

where$\phi_{m,k}$ is the initial phase and $\delta_{m,k}\,(t)$+$\phi_{m,k}$ are the phases in the two locations, and Em,k are the amplitudes of the fields. It should be noted that the phase change, or term $\phi(t) = f(\xi(t))$ is a function of the external perturbation $\xi(t)$ and appears in the expression for the field term for position k but not for position m. The two fields in equation 3.1 interfere with one another because of the source's coherence, and the intensity at the receiver as a result has the following expression:

$$I = E_m^2 + E_k^2 + 2E_m E_k \cos(\Delta\delta(t) + \phi(t))[10] \tag{3.2}$$

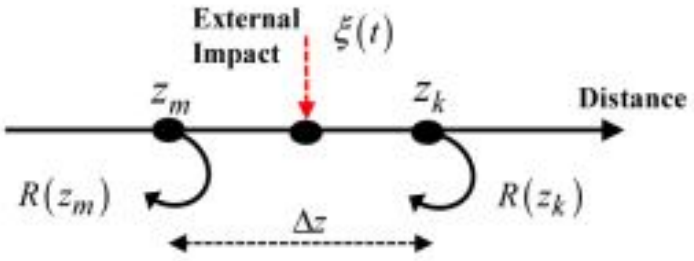

FIGURE 3.1: Schematic of a double pulse Φ-OTDR[3]

where $\phi(t)$ is the relative phase change between the two positions in the presence of the external impact, and $\Delta\delta(t) = C\cos\omega_0 t$, where ω_0 is the modulation angular frequency and C is the modulation depth. As a result,3.2 demonstrates how the double pulse configuration effectively transforms the Φ-OTDR configuration for each spatial point into an interferometer configuration. The phase change brought

about by the external impact information is contained in the beating signal, which can then be extracted using an appropriate demodulation method. To extract the phase, we employ a phase-generated carrier (PGC) demodulation scheme in our suggested method, which is ideal for distributed sensing. By examining the general case of a phase-modulated signal with an arbitrary phase, $\theta(t) = C\cos\omega_0 t + \phi(t)$, which is the phase change in the interfering signal as stated in equation 3.2, the concept of phase extraction using a generic PGC demodulation technique can be explained [23]. When an external impact is present, the detected intensity causes a phase change of $\phi(t)$, which can be expressed as follows:

$$I = A + \eta B\cos(C\cos\omega_0 t + \phi(t))[1] \tag{3.3}$$

A , B, and η are parameters that rely on the optical power input at the receiver. A represents the DC component, B is the amplitude, and η denotes the interferometer's mixing efficiency. Using the cosine of sums property to expand the second term in equation 3.3 results in:

$$I = A + \eta B\{\cos(C\cos\omega_0 t)\cos\phi(t) - \sin(C\cos\omega_0 t)\sin\phi(t)\}[1] \tag{3.4}$$

The term containing a linear multiplication inside the cosine and sine functions can be expanded since the Bessel's expansions of the nested sine and cosine functions are, for any constant C:

$$\cos(C\cos(x)) = J_0(C) + 2\sum_{n=1}^{\infty}(-1)^n J_{2n}(C)\cos(2nx), [1] \tag{3.5}$$

$$\sin(C\cos(x)) = 2\sum_{n=0}^{\infty}(-1)^n J_{2n+1}(C)\cos((2n+1)x), [1] \tag{3.6}$$

where $J_n(C)$ is the n-th order Bessel function of C. The intensity can be expressed as the sum of two terms obtained by substituting the terms in 3.4 and 3.5 in their respective positions in 3.5 and using $x = \omega_0 t$.

$$I = A + \eta B[\Phi_1 + \Phi_2][1] \tag{3.7}$$

The terms Φ_1 and Φ_2 in 3.7 are two orthogonal components given by [23]:

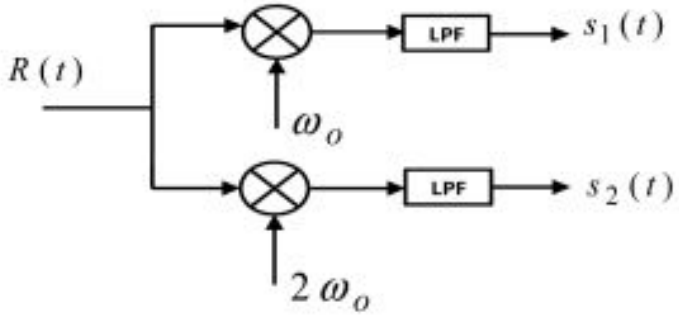

FIGURE 3.2: Initial mixing in PGC demodulation to obtain intermediate signals to the I and Q components.[4]

$$\Phi_1(t) = [J_0(C) + 2\sum_{n=1}^{\infty}(-1)^n J_{2n}(C)\cos(2n\omega_0 t)]\cos\phi(t)[1] \tag{3.8}$$

$$\Phi_2(t) = [2\sum_{n=0}^{\infty}(-1)^n J_{2n+1}(C)\cos((2n+1)\omega_0 t)]\sin\phi(t)[1] \tag{3.9}$$

$$\tag{3.10}$$

3.8, shows that the $\phi_1(t)$ component is non-zero when $\phi(t)$ is zero, whereas the $\phi_2(t)$ equation in 3.8 vanishes. On the other hand, when $\phi(t) = \frac{\pi}{2}$, $\phi_2(t)$ is non zero and $\phi_1(t)$ is eliminated. The first even and odd multiples of ω_0 serve as the center of these signals. It is also important to note that $\phi(t)$ itself can be expanded to give $\phi(t) = D\cos(\omega t)+\xi(t)$ for the generic case of a phase change with amplitude D and angular frequency ω. The two intermediate components in a fiber interferometric system are retrieved using the interference signal at the receiver $R(t)$. This is achieved by combining the incoming signal with two oscillators at ω_0 and $2\omega_0$, then low pass filtering the mixture, as illustrated in Fig.3.6. To obtain the desired phase change, these signals are then processed using a PGC demodulation algorithm. Considering a generic case where the two signals at the receiver in Fig.3.6 have respective carrier amplitudes of G and H and interference visibility of η, these can be written as:

$$\begin{aligned} s_1(t) &= -\eta BGJ_1(C)\sin\phi(t).[1] \\ s_2(t &= -\eta BHJ_2(C)\cos\phi(t).[1] \end{aligned} \tag{3.11}$$

PGC demodulation technique has many advantages such as high resolution, large dynamic range, and strong signal fidelity, so it is widely used in Fiber-optic interferometric sensors(FOIS). There are two main types of demodulation algorithms:

PGC Differential Cross- Multiplication algorithm (PGC-DCM) and the PGC Arctangent algorithm (PGC-Arctan)

3.1.1 PGC-Arctan demodulation

An algorithm known as PGC-Arctan is The inverse tangent of the ratio of the two components is used in the PGC-arctan method, a frequently used scheme. To obtain the phase $\phi(t)$, the PGC arctan algorithm requires that the modulation depth (C) value be such that$J_1(C) = J_2(C)$, which holds true for a value of $C = 2.63$. This can be done by simply calculating the inverse tangent of the ratio of the two terms in 3.11. This condition reduces the demodulated phase to the direct inverse tangent of the ratio of $s_1(t)$ and $s_2(t)$, for equal amplitudes G and H.
The reduction of the amplitudes of two components with a certain ratio yields the negligible influence of Light Intensity Disturbance (LID). Nonetheless, demodulation errors are introduced by any deviation of the modulation depth value from the ideal 2.63. Research has shown that even small deviations from this value can affect the accuracy of phase measurements, so strict adherence to it is not the best way to minimize demodulation errors. Additionally, the method involves phase unwrapping for phase values outside the arctan function's range, which, when combined with the right algorithm, effectively eliminates discontinuities. The computational intensity of multidimensional phase unwrapping, especially in the presence of fast jumps in the instantaneous phase, has been the focus of numerous investigations. While this technique proves to be insensitive to Light Intensity Disturbance (LID), the inherent non-linearity of the arctangent function renders the algorithm more susceptible to demodulation errors. The later-proposed PGC-Arctan algorithm addresses the influence of LID but introduces challenges related to nonlinear distortion due to factors such as carrier phase delay and drift in phase modulation depth (C).

Particularly, when the C value deviates from the optimal 2.63 radians, the PGC-Arctan algorithm exhibits significant harmonic distortion. The C value is dependent on the sinusoidal carrier's amplitude and the parameters of the phase modulator, which are subject to variations in laser wavelength, temperature, and humidity. Consequently, real-time estimation and calibration of fluctuating C values become imperative in practical applications. In essence, refining the algorithm to account for these factors ensures more robust and accurate demodulation in the dynamic and variable conditions encountered in real-world scenarios.
In order to solve the problem of nonlinear distortion in PGC demodulation algo-

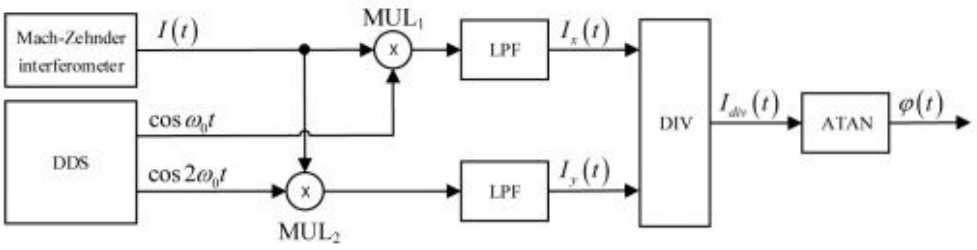

FIGURE 3.3: Phase demodulation in the Φ-OTDR sensor using PGC-Arctan.[5]

rithm, scholars have proposed several methods. Some algorithms only focused on C, for example, J. He et al. presented a PGC demodulation algorithm based on the arctangent function and DSM [12].

3.1.2 PGC-DCM demodulation

The differentiate-and-cross-multiply (PGC-DCM) scheme is another commonly used PGC demodulation technique. In this scheme, the phase is obtained by first differentiating each of the components, $s_1(t)$ and $s_2(t)$, and then cross-multiplying them before calculating their difference. Using the trigonometric identity and this scheme applied to the intermediate components in 3.11, we first obtain[24]:

$$\begin{aligned} s_{DCM}(t) &= [B^2\eta^2 GHJ_2(C)J_1(C)] \times [\sin^2\phi(t) + \cos^2\phi(t)]\phi(t)[1] \\ &= B^2\eta^2 GHJ_2(C)J_1(C)\phi(t) \end{aligned} \tag{3.12}$$

The final phase multiplied by the remaining terms is obtained by integrating the final term in 3.12:

$$s_{DCM}(t) = B^2\eta^2 GHJ_2(C)J_1(C)\phi(t)[1] \tag{3.13}$$

The main problem with the PGC-DCM technique, as 3.13 shows, is that the demodulated phase clearly depends on the square of the B value and mixing efficiency η, even though the Bessel function terms of the modulation depth are just simple linear multiplicities. This results in large demodulation errors and detrimental light intensity disturbance (LID), which calls for methods like normalizing—which introduces distortions—or tracking the intensity and utilizing feedback loops to reduce [13]. Hence, the PGC-DCM is appropriate for distributed measurements because it doesn't require complex phase unwrapping algorithms. Studies have

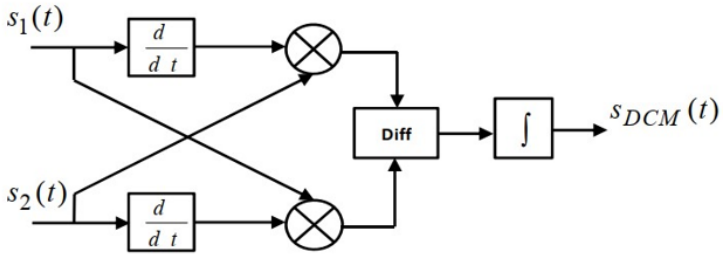

FIGURE 3.4: Phase demodulation in the Φ-OTDR sensor using PGC-DCM.[6]

also shown that PGC-DCM is robust against undesirable harmonic distortions, which are high when using the PGC-arctan method and the modulation depth deviates from its nominal value [24]. Since there are no division operations, the method is also suitable for situations where one of the intermediate signals used to obtain the demodulated phase has several zero-crossing points thereby avoiding additional mechanisms to mitigate division-by-zero operations. The other interesting feature of the demodulation technique is that the PGC-DCM algorithm also involves symmetric differentiation and integration operations which are particularly suitable for analog processing systems. Thanks mainly to the rich set of techniques for fractional order calculus [25], which has applications in a number of control systems, efficient implementations of the integration and differentiation computations have already been implemented using FPGA and analog processing systems [26]. In a distributed sensing scheme, FPGA-based signal processing can easily be implemented in an efficient system that involves concurrent computations on multiple channels corresponding to different sensing locations along the sensing fiber.

3.1.3 PGC-DMS demodulation

Another PGC demodulation algorithm is the Differentiate-Multiply Square (PGC-DMS) technique, the basic workings of which are illustrated in [24]. As demonstrated, to extract the instantaneous phase from the intermediate components, it suffices to differentiate $s_1(t)$, multiply the result by $s_2(t)$, and divide the resulting value by the square of$s_2(t)$. Applying the product and square terms to the two intermediate terms at the receiver provided in 3.11 results in the following:

$$\begin{aligned} s_{D1}(t)s_2(t) &= (\eta B)^2 GHJ_1(C)J_2(C)\cos^2\phi(t)\frac{d}{dt}\phi(t), [10] \\ s_{SQ2}(t) &= (\eta BH)^2 J_2^2(C)\cos^2\phi(t) [10] \end{aligned} \tag{3.14}$$

Taking the ratio of the terms in 3.14 and assuming that G and H have equal amplitudes in the mixing carriers, we get:

$$\frac{s_{D1}(t)s_2(t)}{s_{SQ2}(t)} = \frac{J_1(C)}{J_2(C)}\frac{d}{dt}\phi(t).[10] \tag{3.15}$$

Similar to the PGC-DCM case, the instantaneous phase will have the form $\phi(t) = D\cos(\omega t) + \xi(t)$ since it includes both the high frequency perturbation and the low frequency environmental drift. Therefore, to obtain any phase change, integrate 3.15 first, and then, if necessary, high-pass filter the result to eliminate slow environmental drifts:

$$S_{DMS}(t) = \int \frac{J_1(C)}{J_2(C)}\frac{d}{dt}\phi(t)dt = \frac{J_1(C)}{J_2(C)}\phi(t)[10] \tag{3.16}$$

As is evident from 3.16, both terms B and η which are challenging to control—are eliminated when using the PGC-DCM algorithm, and the ratio of the two Bessel functions for any value of the modulation depth C remains merely a linear multiplication factor. The phase demodulation results would be considerably impacted by this method's strong suppression of the LID. In comparison to the PGC-arctan and PGC-DCM approaches, it is shows improved suppression of the total harmonic distortion [24]. Note that mind that the presence of disturbance in light intensity. due to backscattering signal fluctuations is a problem in many of the Φ-

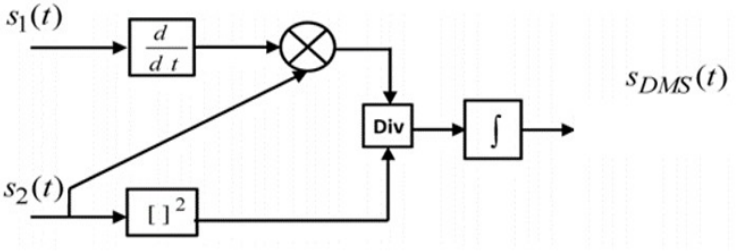

FIGURE 3.5: Phase demodulation in the Φ-OTDR sensor using PGC-DMS.[4]

OTDR demodulation techniques currently in use and needs to be suppressed with additional techniques. Owing to the division operation which cancels the common terms, the PGC-DMS is robust against changes in the signal's intensity at the receiver.

3.2 Fast Hilbert transform

The Hilbert transform is widely used in signal processing and is one of the most important operators in signal theory. It is named after David Hilbert (1862-1943). Its first use dates back to 1905 in Hilbert's work concerning analytical functions concerning the Riemann problem. In 1928 it was proved by Marcel Riesz (1886-1969) that the Hilbert transform is a bounded linear operator on Lp(R) for $1 < \rho < 1$. This result was generalized for the Hilbert transform in several dimensions (and singular integral operators in general) by Antoni Zygmund (1900-1992) and Alberto Calderon (1920-1998). Mainly, the importance of the transform is due to its property to extend real functions into analytic functions [27]. The other important demodulation technique for band-limited signals is the one which utilizes the Hilbert transform. For any function $u(t)$, the Hilbert transform denoted by $H(u(t))$ is given by [28]:

$$-H[u(t)] = \frac{1}{\pi}\int_{-\infty}^{\infty}\frac{u(x)}{t-x}dx, [29] \tag{3.17}$$

which can also be expressed as a convolution of two functions:

$$H[u(t)] = u(t) * \frac{1}{\pi t}[29] \tag{3.18}$$

The Fourier transform of the Hilbert transform is given by:

$$U(\omega) = X(\omega)[-jsgn(\omega)][29] \tag{3.19}$$

where $sgn(\omega)$is a function defined as:

$$Sgn(\omega) = \begin{cases} 1, \omega > 0 \\ 0, \omega = 0 \\ -1, \omega < 0[29] \end{cases} \tag{3.20}$$

To use the Hilbert transform for phase modulation, consider a band-limited signal v(t) which is phase modulated onto a carrier with frequency ω_c to obtain a modulated waveform:

$$s(t) = Acos[\omega_c t + kv(t)], [29] \tag{3.21}$$

where A is the amplitude of the modulated signal, and k is the modulation index. Considering the Hilbert transform of $\cos(\theta(t))$ is $\sin(\theta(t))$, the perturbation inside

the phase term can be calculated from 3.22:

$$\omega_c + kv(t) = \arctan\left[\frac{H(s(t))}{s(t)}\right], [29] \tag{3.22}$$

and becomes:

$$v(t) = \frac{\arctan\left[\frac{H(s(t))}{s(t)}\right] - \omega_c t}{k}. [29] \tag{3.23}$$

In this work, we investigate the impact of using the aformentioned demodulation techniques on the overall computation time for different ranges of sampling points corresponding to representative sensing distance ranges in a DAS monitoring scenario. All PGC-based demodulation techniques involve pre-processing with mixing and low-pass filtering of the input interferometric signal. Considering this, the computations in the PGC-based demodulation algorithms were made consistent among each other. The same approach was taken for the arctan implementation for both demodulation using Fast Hilbert Transform (FHT) and PGC-arctan, so that a fair comparison of the computation time performance can be made, as the former only operates on the input signal without pre-processing via mixing and low pass filtering involved in all the PGC.

3.3 Dynamic measurements based on a Fast Hilbert Transform (FHT)

The phase-generated carrier (PGC) technique is a commonly used phase demodulation technique in both point interferometric and distributed dynamic sensors. It is based on an unbalanced interferometer in which the phase-modulated signal is divided into two arms, and one of them is selectively phase modulated with a known frequency ω_0 and amplitude C. Then the resulting signal is mixed with sinusoidal at predetermined frequencies ω_0 and $2\omega_0$, and low pass filtered to obtain two scaled intermediate signals which $S1$ and $S2$, which constitute orthogonal components of the desired signal scaled with the mixing amplitudes and efficiencies as well as $J1(C)$ and $J2(C)$ which are Bessel functions of the modulation depth C.

3.4 LabVIEW software

LabVIEW (abbreviation for Laboratory Virtual Instrument Engineering Workbench) is National Instruments' (NI) system design platform and visual programming language development environment. Widely used in data acquisition, equipment control, and industrial automation, in academic, research, and industrial development environments due to its versatility and ease of use. National Instruments' LabVIEW is the industry-leading software tool for designing test, measurement, and control systems. Since its introduction in 1986, engineers and scientists around the world have relied on NI LabVIEW graphics development for projects across the product design cycle to improve quality, reduce time to market, and design and manufacturing efficiency. It also enhances productivity across organizations by using the integrated LabVIEW environment to manipulate real-world signals, analyze data for meaningful information, and share results. In addition, LabVIEW provides the flexibility of a programming language combined with built-in tools specifically designed for test, measurement and control, allowing system engineers to create applications ranging from simple temperature monitoring to advanced simulation and control systems.[30]

3.4.1 Key Features and Components:

- Graphical Programming Language: LabVIEW uses a graphical programming language called G, where users create programs by connecting icons (VIs - Virtual Instruments) on the block diagram.
- Virtual Instruments (VIs) VIs are the building blocks of LabVIEW programs. They can be functions, subroutines, or control and display elements.
- Front Panel and Block Diagram: The LabVIEW interface consists of two main parts: the front panel, where user interfaces and controls are placed, and the block diagram, where the VI's functionality is defined graphically.
- Data flow Programming: LabVIEW operates on a data flow programming model, where the flow of data controls the execution of the program. Each VI only runs when data is available to it.
- Instrument Connectivity: LabVIEW supports a wide range of hardware interfaces and protocols, making it suitable for controlling and acquiring data from various instruments and devices.

Data Acquisition and Analysis:

- LabVIEW includes tools for data acquisition, signal processing, and analysis. It is commonly used in applications involving sensors, DAQ (Data Acquisition), and real-time measurements.
- Integration with External Tools: LabVIEW integrates with other programming languages and tools. For example, it can call and be called from other programming languages such as C/C++, .NET, MATLAB,Python, etc...
- Application Development: LabVIEW is used to create applications for various purposes, from simple control systems to complex measurement and automation systems.
- Modularity and Reusability: VIs can be easily created, modified, and reused, promoting modularity and efficient development practices.
- Real-Time and FPGA Modules: LabVIEW Real-Time and LabVIEW FPGA modules extend the capabilities of LabVIEW to run on real-time hardware and FPGA (Field-Programmable Gate Array) devices, respectively.
- Community Support: LabVIEW has a strong community of users, and National Instruments provides extensive documentation, forums, and tutorials to support users.

3.4.2 Applications

- Test and Measurement: LabVIEW is commonly used for creating automated test systems and conducting measurements in laboratory settings.
- Control Systems: It is employed in the development of control systems for a variety of applications, from industrial automation to research experiments.
- Data Logging and Analysis: LabVIEW is used for real-time data logging, analysis, and visualization.
- Simulation: The software supports the simulation of systems, which is valuable in the design and testing of various applications.
- Educational Purposes: LabVIEW is widely used in educational institutions for teaching and learning purposes in engineering and science fields.

Hence, LabVIEW is a powerful tool with a broad range of applications, and its user-friendly graphical programming approach makes it accessible to users with varying levels of programming experience. in the figure below 3.6 and 3.7, we will see the front panel and block diagram of LabVIEW software.

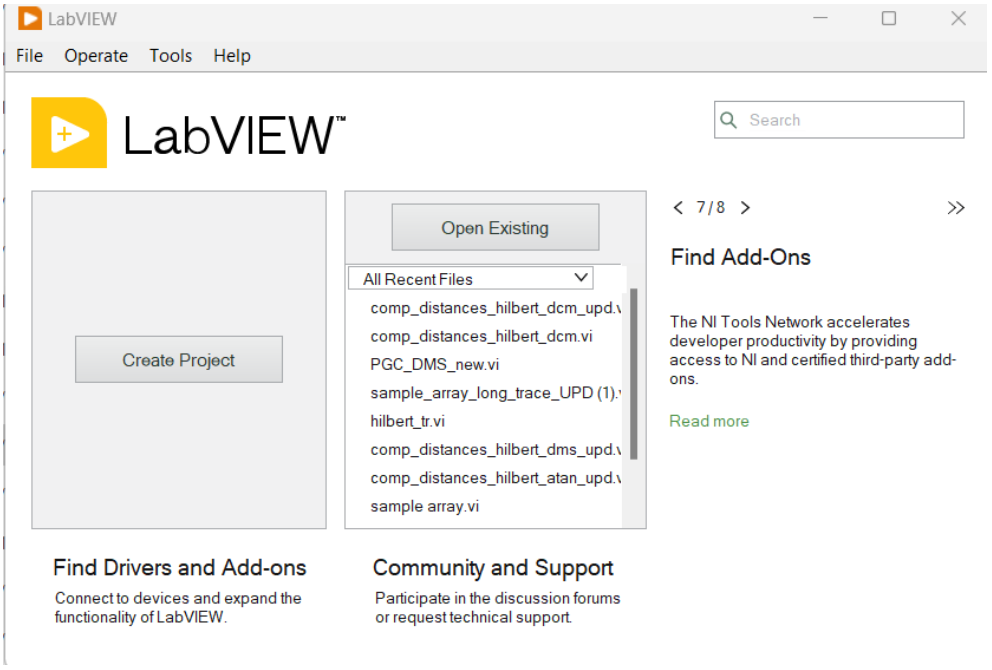

FIGURE 3.6: LabVIEW first page

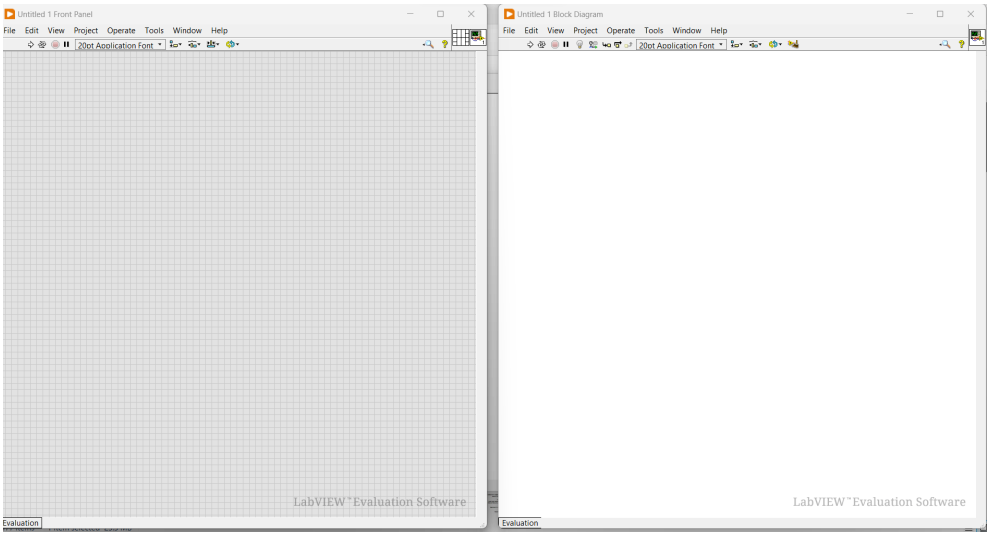

FIGURE 3.7: the front panel and block diagram of LabVIEW software

LabVIEW uses a large amount of processing power and computer memory, thus requiring a powerful computer. A large-screen monitor is desirable when developing larger applications. LabVIEW is excellently suited by testing new monitoring paradigms, analysis algorithms, or user interfaces[31].

Chapter 4

Result and Discussion

This chapter presents and discusses the study's results in the context of the research questions. The findings are analyzed, and their implications are explored, providing a comprehensive understanding of the research outcomes. Real-time applications in signal processing depend heavily on an algorithm's computing efficiency. There are a few steps involved in using LabVIEW's Fast Hilbert Transform demodulation algorithms for distributed acoustic sensors. Here are the steps:

- Signal Generation: Create a LabVIEW VI for generating acoustic sensor signals. This involves simulating and acquiring real-world data from distributed sensors.

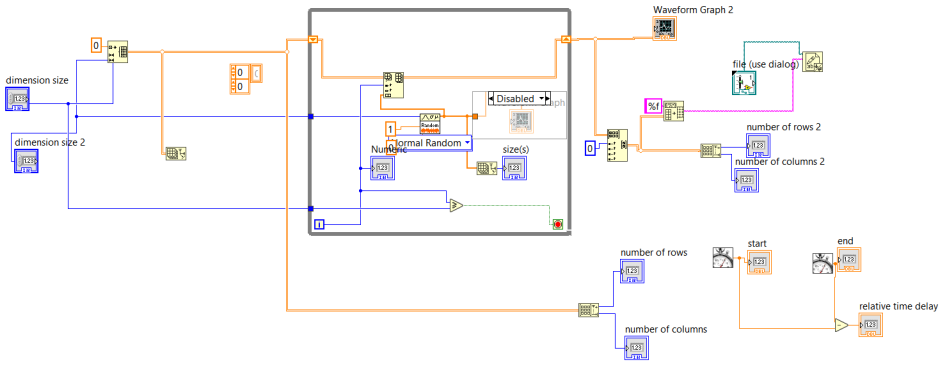

FIGURE 4.1: Sample array generation with random values for backscattering signal

- Fast Hilbert Transform (FHT): Implement the PGC-arctan, PGC-DMS, PGC-DCM as and FHT-based demodulation algorithms, the latter by transforming time-domain signals into their analytic representations and applying

the FHT to demodulate the signals. The demodulation process helps extract features from the signals.

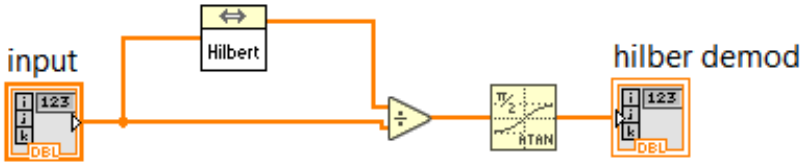

FIGURE 4.2: Implementation Fast Hilbert Transform

- Signal Analysis: Real-time monitoring for evaluation and validation of the performance of the demodulation algorithm in terms of computation times for multiple scenarios.

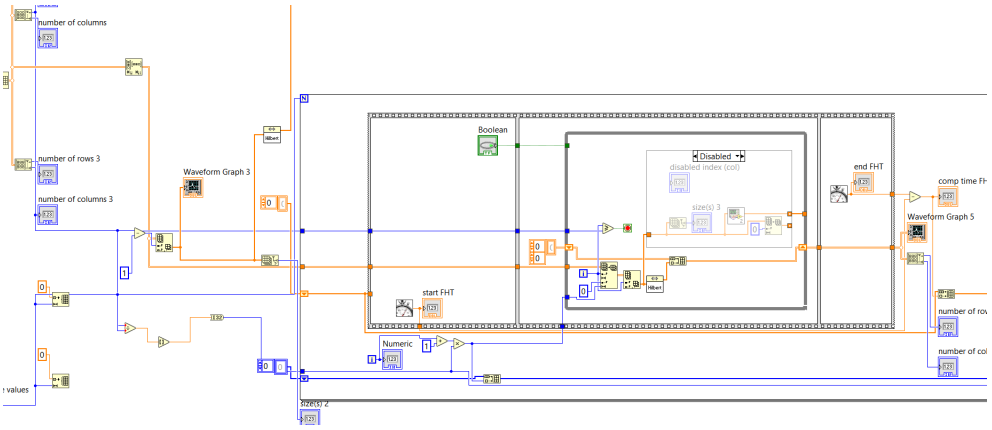

FIGURE 4.3: calculation of computation times in Fast Hilbert Transform

4.1 PGC-arctan vs FHT

Our initial performance assessment involved comparing the computation times of PGC-arctan and the Hilbert transform on a sample block of backscattering traces representing phase-modulated data in a monitoring scenario. Initially, we considered 1000 consecutive traces, each with varying sampling point as shown in Figure 4.7 for PGC-arctan in LabVIEW. To conduct a comprehensive evaluation,

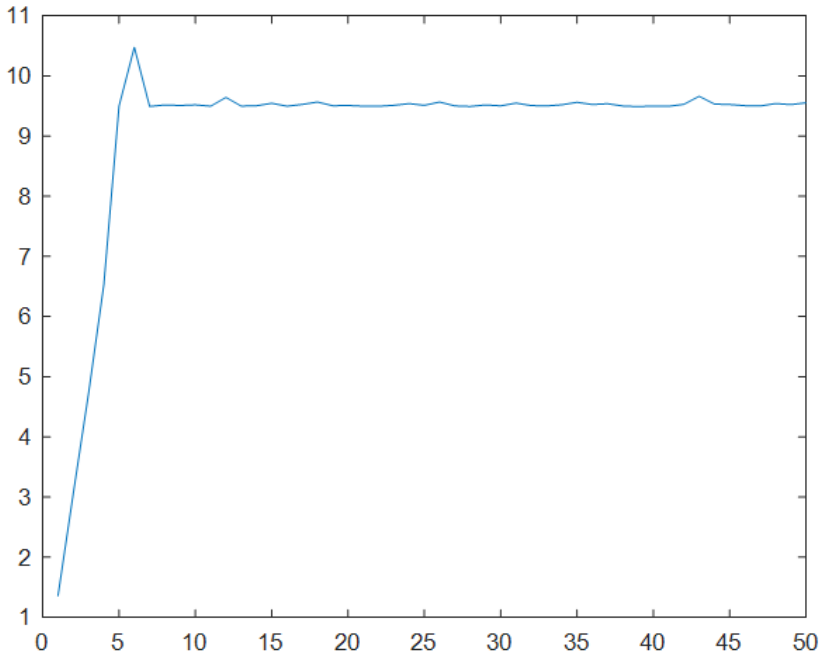

FIGURE 4.4: computation times in PGC-arctan demodulation for 50 different sampling points

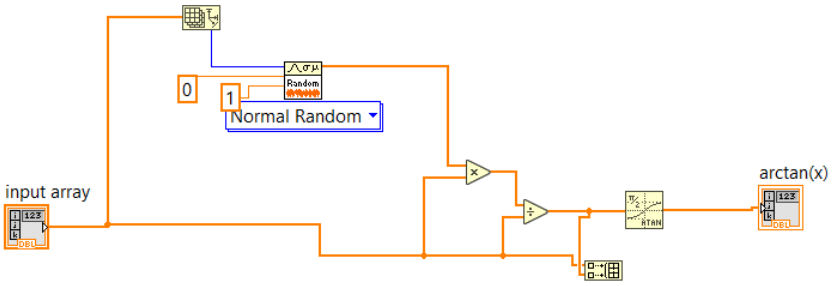

FIGURE 4.5: sample block of PGC-arctan demodulation

the number of acquired traces were kept constant while varying the number of sensing points for demodulation using both the arctan demodulation and Hilbert transform functions. The computation times for each method were recorded over 10 subsequent runs, and the results are presented in figure 4.6.

Figure 4.6 illustrates a substantial reduction in computation times when employing phase demodulation with FHT compared to PGC-arctan. The reduction is approximately three orders of magnitude compared to the PGC-arctan method. This improvement in efficiency suggests that the Fast Hilbert transform is highly

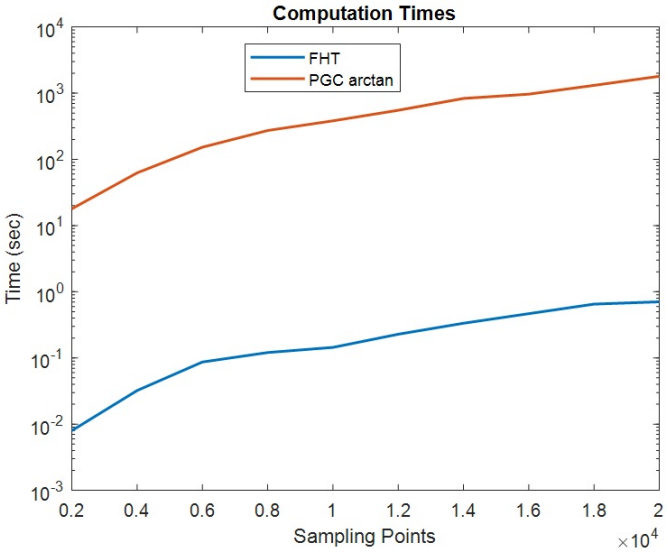

FIGURE 4.6: Comparisons of computation times for varying sampling points for FHT and PGC-arctan demodulation

advantageous for processing phase-modulated data in this monitoring scenario. These findings underscore the practical benefits of adopting the Fast Hilbert transform for applications involving backscattering traces and phase-modulated data. The enhanced computational efficiency opens up opportunities for real-time or resource-constrained environments where rapid data processing is crucial. Further analysis and experimentation may reveal additional insights into the specific conditions under which the Fast Hilbert transform excels, contributing to its broader applicability in distributed monitoring scenarios.

4.2 PGC-DCM, PGC-DMS VS FHT

Because measurement in long-distance DAS consists in extracting information from thousands of sensing points along the fiber, when real-time responsiveness is required, it is critical to examine how long the different demodulation algorithms take for sensing over the entire span. In addition to guaranteeing the prompt extraction of acoustic vibration throughout the fiber optic network, this study enables engineers to spot any bottlenecks and regions in need of development. The complexity of fiber optic communication systems necessitates careful analysis of calculation time to achieve the ideal ratio of accuracy to productivity. Sensing system developers can modify the PGC-DMS system to fulfill the demanding requirements of distributed acoustic sensing in dynamic fiber optic settings by improving the system's functionality and dependability in practical applications.

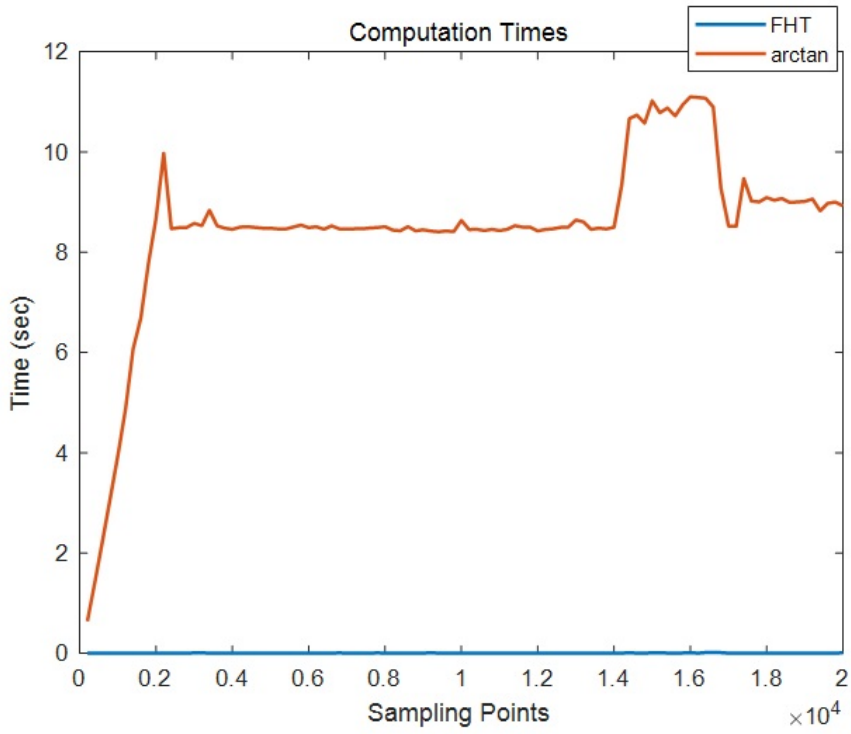

FIGURE 4.7: Comparisons of computation times for varying sampling points for FHT and PGC-arctan 100 demodulation

This can be achieved by improving the LabVIEW implementation and algorithmic procedures. The schematic of LabVIEW implementations of PGC-DCM and PGC-DMS algorithms are depicted in figures 4.8and 4.12.

To compare the efficiency of FHT with PGC-DCM and PGC-DMS the blocks shown in Figure 4.8 and 4.12 were used.

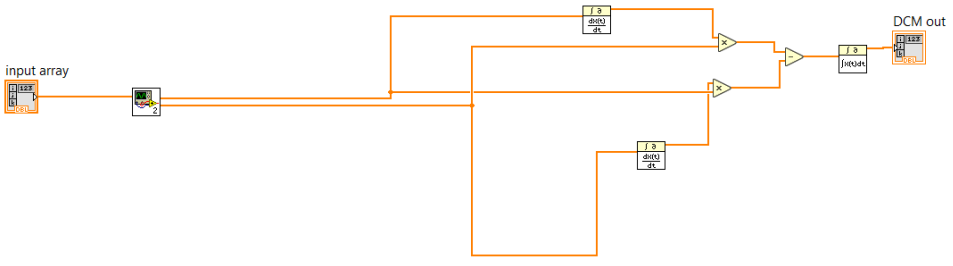

FIGURE 4.8: sample block of PGC-DCM demodulation

The computation times for both the PGC-DCM and PGC-DMS algorithms were systematically evaluated across 100 different numbers of samples. The comparison

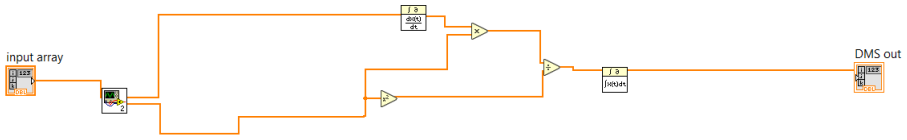

FIGURE 4.9: sample block of PGC-DMS demodulation

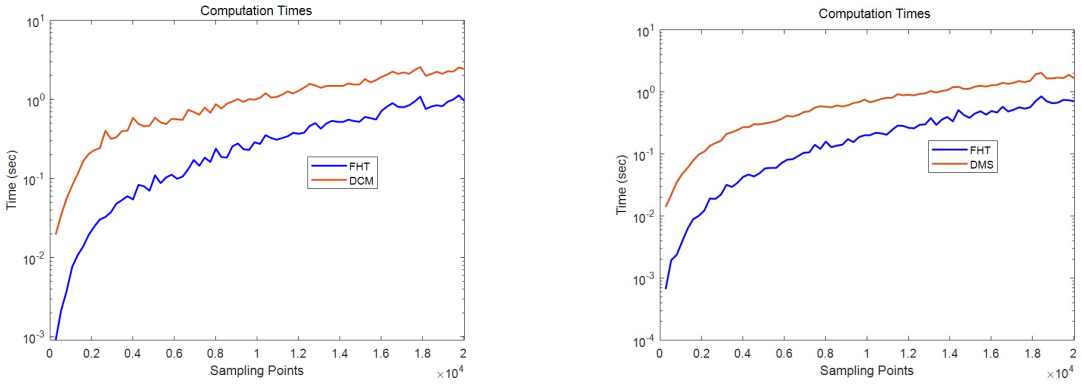

((A)) ((B))

FIGURE 4.10: Comparisons of computation time for phase demodulation for 75 different values of the sending distance for (a) FHT vs PGC-DCM and (b) FHT vs PGC-DMS algorithms

of these results with demodulation using the Fast Hilbert Transform (FHT) under identical processing conditions is visualized in figures 4.10(a) and 4.10(b). Initially, a consistent trend is observed, featuring an initial phase of transition from a lower value up to approximately 2000 samples. Beyond this point, a distinct pattern emerges, highlighting the significantly reduced computation times achieved with the FHT in comparison to both PGC techniques. It is crucial to emphasize that the performance comparison in both cases is computed under uniform conditions of CPU and memory occupancy for both the FHT and PGC methods. This ensures a fair and unbiased assessment of the computational efficiency of each algorithm.

The observed reduction in computation times with the FHT underscores its superiority in handling demodulation tasks, especially when confronted with larger data sets. This improvement can be pivotal in scenarios where real-time processing or efficient resource utilization is required. In summary, the results clearly illustrate the advantages of FHT-based demodulation over traditional PGC techniques across varying sample sizes in terms of dynamic performance. These findings contribute valuable insights into the optimization of demodulation algorithms for applications requiring precision and computational efficiency. To validate and reinforce the advantages of the Fast Hilbert Transform (FHT) across a broader

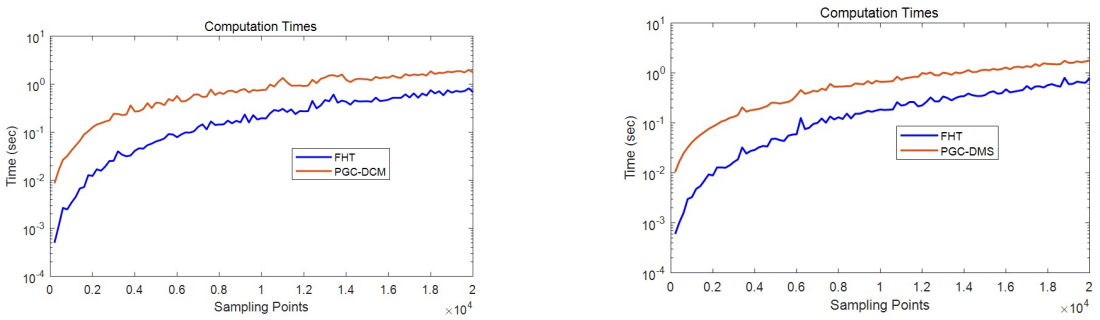

((A)) ((B))

FIGURE 4.11: Comparisons of computation time for phase demodulation for 100 different values of the sending distance for (a) FHT vs PGC-DCM and (b) FHT vs PGC-DMS algorithms

range of distance measurements in a distributed measurement scenario, additional measurements were conducted by expanding the number of sensing distance ranges to 100 points. The results of these extended experiments are reported in Figures 4.11(a) and 4.11(b), further emphasizing the favorable performance of FHT.

The observed advantages of FHT in having consistently lower processing times over a larger number of sensing distance ranges underscore its versatility and efficiency in scenarios where distributed measurements are essential. The smaller average computation times suggest that FHT is not only advantageous for specific conditions but maintains its superior performance across a wide spectrum of sampling points. This validity makes FHT a compelling choice for demodulation in applications demanding real-time responsiveness and reliable performance.

In conclusion, the extended measurements presented in 4.11(a) and 4.11(b) provide additional evidence supporting the advantages of FHT, reaffirming its suitability for demodulation in distributed measurement scenarios, especially in the context of real-time monitoring applications.

The experiment was replicated with random memory occupancy and concurrent processing with other applications, and the computation times for all algorithms are presented in 4.12, which shows the computation times in logarithmic scale. Not fixable, due to substantial delays introduced by the PGC-arctan method, the comparison window was restricted to a maximum of 1800 seconds for this particular method.

4.3 All VS FHT

The computation time using the FHT algorithm for the maximum sensing distance is consistently lower by a factor of 3.04 when compared to both the DCM and DMS techniques. Furthermore, the DCM and DMS techniques demonstrate comparable performance, both significantly outperforming the PGC-arctan method. Specifically, at 20,000 samples, the FHT method achieves a remarkable reduction in computation time by nearly three orders of magnitude compared to the PGC-arctan method. Additionally, the PGC-arctan method exhibits computation times approximately 838 times higher than both the PGC-DMS and DCM techniques. It's crucial to note that despite both FHT and PGC-arctan methods utilizing the

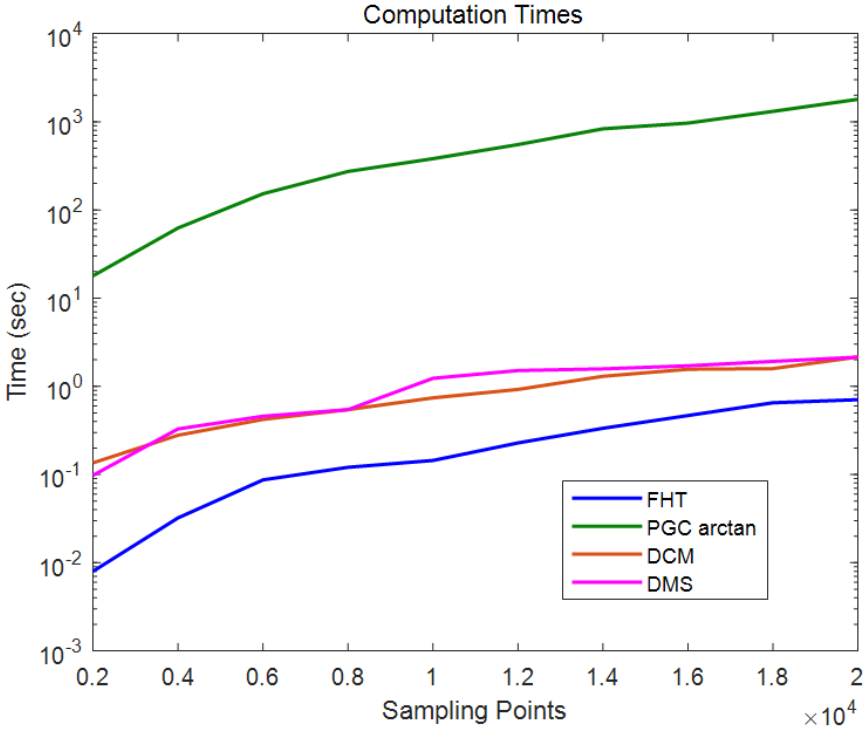

FIGURE 4.12: Comparison of the computation times of the three PGC-based demodulation methods with the FHT algorithm.

arctan function in their phase demodulation processes, the FHT method outshines the PGC-arctan method in terms of computational efficiency. This outcome underscores the limitations of the commonly employed digital mixing and filtering PGC-arctan demodulation, particularly when fast demodulation is essential in real-time measurements within a distributed scenario.

In summary, the findings emphasize the substantial benefits of employing FHT-based demodulation, even when incorporating the arctan function. The results

underscore the inadequacies of PGC-arctan demodulation, especially in the context of real-time measurements in distributed scenarios, further emphasizing the efficiency and suitability of FHT-based demodulation. The enhanced computational efficiency achieved through the Fast Hilbert Transform (FHT) in our model stems from its adept implementation, primarily leveraging the Fast Fourier Transform (FFT). In our National Instruments LabVIEW application, the sequence of operations is such that, initially, the FFT is applied to the input signal, providing a frequency domain representation. Subsequent adjustments involve setting the DC component to zero and nullifying the Nyquist component for even-numbered sequences. The positive frequency components undergo multiplication by $-j$, and the negative counterparts by j, an operation equivalent to multiplying the FFT by $-j * sign(\omega)$. The manipulated signal then undergoes an inverse Fourier transformation to yield the Hilbert transform. Importantly, this methodology is not confined to LabVIEW, as referenced in [29] and [32], where signal processing implementations across diverse applications benefit from parallel computations and multiple processing threads. This parallel processing is particularly advantageous when handling matrices of consecutive traces representing backscattering from various sensing points. In summary, the integration of FHT, FFT, and parallel processing strategies contributes significantly to the reduction in computation time, thereby enhancing the overall efficiency and precision of signal processing in diverse contexts. Beyond the specifics of LabVIEW, the effectiveness of the FHT-FFT combination underscores its versatility across various computational environments. In essence, the amalgamation of FHT, FFT, and parallel processing not only expedites computation but also fortifies the accuracy of signal processing in a myriad of applications. The orchestrated sequence of operations, tailored adjustments, and parallelized computations collectively contribute to an overarching optimization of computational efficiency, making this methodology a robust choice for diverse signal processing scenarios.

Chapter 5

Conclusion and Recommendations

5.1 Conclusion

In this research, we have evaluated the performance of various phase demodulation techniques within the context of Distributed Acoustic Sensing (DAS) applications. The primary criterion under scrutiny has been the computation times associated with these techniques, a critical factor in determining their suitability for real-time demodulation schemes in DAS setups.

Our analysis has shed light on the efficiency of different methods, with a specific emphasis on the Fast Hilbert Transform (FHT) and its comparison to other prevalent techniques such as Phase Generated Carrier (PGC) with Differential Mean Square (DMS), PGC with Differential Cross-Multiply (DCM), and the conventional PGC with arctan method.

Notably, the FHT has emerged as a standout performer regarding response time, exhibiting significantly reduced computation times. The mean values recorded for FHT are significantly low, approximately three times faster than both PGC-DMS and PGC-DCM techniques. Perhaps even more noteworhy is the fact that the FHT method outpaces the commonly used PGC-arctan method by about three orders of magnitude, highlighting a substantial leap in computational efficiency.

The ubiquity of Field-Programmable Gate Array (FPGA)-based implementations for the Fast Fourier Transform (FFT) and inverse FFT operations, integral components of the FHT, has noteworthy implications. This implies that the adoption

of FHT-based phase demodulation schemes is not only feasible but also advantageous in real-time monitoring scenarios, especially those involving distributed sensors.

The implications of our findings extend beyond mere computational efficiency. They point to the need to reconsider the dynamic performance of real-time demodulation algorithms in distributed fiber sensors. Specifically, incorporating FHT-based phase demodulation into DAS systems can potentially unlock enhanced performances in terms of speed, responsiveness, and overall performance. This is particularly relevant in applications where timely and precise monitoring is imperative, such as in structural health monitoring, perimeter security, and environmental sensing. The implications of opting for an FHT-based phase demodulation approach are significant, particularly not just in the realm of Distributed Acoustic Sensing (DAS) but also other quasi-distributed sensors requiring phase demodulation.

- Enhanced Real-Time Monitoring: The reduced response times observed with FHT-based demodulation makes it suitable for real-time monitoring capabilities, in scenarios where rapid and precise data analysis is crucial.
- Resource Optimization: The inherent efficiency of FHT, especially when implemented on FPGA platforms, translates to optimized resource utilization. This not only contributes to faster computations but also allows for the allocation of resources to other critical tasks within the distributed sensor network.
- Scalability and Adaptability: The scalability of FHT-based demodulation schemes is a key feature. As distributed sensor networks grow in complexity and scale, the adaptability of FHT ensures that the computational demands can be met without compromising on real-time performance.
- Versatility in Applications: The applicability of FHT extends across various domains, from structural health monitoring to geophysical sensing. Its versatility positions it as a valuable tool for diverse applications, where the timely extraction of phase information is fundamental to making informed decisions.
- Reduced Latency in Critical Situations: In time-sensitive applications, such as emergency response systems or security monitoring, the ability of FHT to deliver rapid results ensures that critical events are identified and acted upon promptly.

- Scalability of DAS Systems: As technology evolves, the integration of FHT aligns with the trajectory of advancements in distributed sensing. Scalability of DAS systems with FHT-based demodulation ensures that these systems remain ubiquitous and get readily incorporated into emerging technologies.
- Cost-Efficiency: The efficiency gains achieved with FHT may also translate into cost savings. Faster computations mean that the computational infrastructure, whether in terms of hardware or cloud resources, can be optimized for cost-effectiveness without sacrificing performance.

In summary, further investigation and adoption of FHT-based phase demodulation techniques represents a signifiant step in the evolution of distributed sensors, particularly in the context of DAS applications. The benefits span beyond mere computational efficiency, encompassing resource optimization, scalability, versatility, and adaptability. As we look to the future, the integration of FHT emerges as a critical choice for those seeking to elevate the dynamic performance and scalability of distributed sensor systems across a spectrum of applications. Our investigation reveals the comparative performance of phase demodulation techniques and highlights the benefits of further study and experimental verifications of phase extraction using FHT-based demodulation in DAS.

5.2 Recommendations

In light of our comprehensive investigation into the performance of various phase demodulation techniques, particularly in the context of Distributed Acoustic Sensing (DAS) applications, several key recommendations emerge.

To fully capitalize on the computational efficiency of FHT, we recommend integrating this approach with Field-Programmable Gate Array (FPGA) platforms. FPGA-based implementations of the FFT and inverse FFT operations, integral to FHT, offer a practical and efficient solution, ensuring optimal resource utilization.

Consideration for Dynamic Environments: In applications where environmental conditions are dynamic and rapidly changing, such as structural health monitoring or industrial process control, the use of FHT-based demodulation is particularly advantageous. Its reduced latency and enhanced real-time capabilities make it well-suited for scenarios where timely responses are critical.

Scalability and Future-Proofing: Researchers working on distributed sensing systmes should consider the scalability and adaptability of FHT-based demodulation schemes. This approach ensures that the computational demands can be met as the network grows, future-proofing the system against evolving requirements and emerging technologies.

Our recommendations emphasize the strategic adoption of FHT-based phase demodulation, thoughtful integration with FPGA platforms, consideration for dynamic environments, scalability, cross-disciplinary applications, investment in training, and continuous monitoring of technological advancements. By following these recommendations, organizations can harness the full potential of FHT to elevate the performance and capabilities of their distributed sensor networks.

5.2.1 Future Work

In the pursuit of advancing the field of phase demodulation within distributed sensing applications, several avenues for future work present exciting opportunities for research and development. Here are some potential directions for future work:

- Algorithmic Refinements: Further exploration and refinement of the FHT-based demodulation algorithm can uncover opportunities for optimization and performance enhancements. Investigating algorithmic tweaks or variations could lead to improvements in computational efficiency and overall responsiveness.
- Hybrid Techniques Integration: Exploring hybrid approaches that integrate FHT with other demodulation techniques or signal processing methods could yield synergies. Combining the strengths of different approaches may lead to enhanced robustness and adaptability, especially in challenging and dynamic sensing environments.
- Adaptive FHT Implementations: Developing adaptive FHT implementations that can dynamically adjust parameters based on changing environmental conditions or signal characteristics is a promising avenue. This adaptability could improve the resilience of FHT-based demodulation in diverse and unpredictable scenarios.
- Machine Learning Integration: Investigating the integration of machine learning models for pattern recognition and anomaly detection within the FHT-based demodulation framework holds considerable potential. This could provide an intelligent layer for automated decision-making and early identification of unusual events.
- Hardware Acceleration Techniques: Exploring advanced hardware acceleration techniques, beyond FPGA platforms, such as Graphics Processing Units (GPUs) or specialized accelerators, can further optimize the execution speed of FHT-based demodulation. This is particularly relevant in scenarios where real-time processing is critical.
- Application-Specific Implementations: Tailoring FHT-based demodulation implementations for specific applications or industries, such as healthcare, structural engineering, or environmental monitoring, can lead to specialized solutions. Customizing the algorithm to address the unique requirements of each application domain enhances its practical utility.

- Distributed Sensor Network Scalability: Investigating the scalability of FHT-based demodulation in larger and more complex, multi-parameter distributed sensor networks is crucial. Understanding how the algorithm performs as the number of sensors or data points increases will provide insights into its feasibility for extensive deployment.
- Real-Time Visualization Tools: Developing intuitive and real-time visualization tools that accompany FHT-based demodulation results can enhance user understanding and decision-making. Interactive interfaces that allow users to explore and interpret the demodulated data in real-time can be valuable in practical applications.

As researchers delve into these future directions, the collective knowledge gained will contribute to further improvement of FHT-based demodulation techniques and their integration into various distributed sensing systems employed in many critical safety and integrity monitoring systems. The interdisciplinary nature of these advancements will enable more impactful progress in the area.

Appendix A

Codes

```
plot (output1(1,:), 'LineWidth', 1.5);
hold on;
plot (output1(2,:), 'LineWidth', 1.5);
legend ("FHT", "arctan");
%xmin=0;
%xmax=2.5E-4;
%ymin=-4.8369;
%ymax=-4.83684127238243;
%axis([xmin xmax ymin ymax]); %x-axis limit is from 0 to 5, y-axis
   limit is from 0 to 50

title('Computation Times');
xlabel('Sample');
ylabel('Time (sec)');
hold off
```

Listing A.1: hilbert atan polt

```
output1= input1;

plot (samp_points, output1(1,:), 'LineWidth', 1.5)
hold on;
plot (samp_points, output1(2,:), 'LineWidth', 1.5);
legend ("FHT", "DMS");
%xmin=0;
%xmax=2.5E-4;
%ymin=-4.8369;
```

```
%ymax=-4.83684127238243;
%axis([xmin xmax ymin ymax]); %x-axis limit is from 0 to 5, y-axis
   limit is from 0 to 50

title('Computation Times');
xlabel('Sampling Points');
ylabel('Time (sec)');
hold off

% for number distance 100 uses this
%mean_steady_state_hilbert= mean (output1(1, 90:100))
%mean_steady_state_dms= mean(output1(2, 90:100))

%for number of distances N, use ouptut(1, N-10: N) and, ouput(2, N
   -10: N)

mean_steady_state_hilbert= mean (output1(1, 5:10))
mean_steady_state_dms= mean(output1(2, 5:10))
```

LISTING A.2: hilbert dms polt

```
output1= input1;

plot (samp_points, output1(1,:), 'LineWidth', 1.5)
hold on;
plot (samp_points, output1(2,:), 'LineWidth', 1.5);
legend ("FHT", "DCM");
%xmin=0;
%xmax=2.5E-4;
%ymin=-4.8369;
%ymax=-4.83684127238243;
%axis([xmin xmax ymin ymax]); %x-axis limit is from 0 to 5, y-axis
   limit is from 0 to 50

title('Computation Times');
xlabel('Sampling Points');
ylabel('Time (sec)');
hold off
output1= input1;
```

```
plot (samp_points, output1(1,:), 'LineWidth', 1.5)
hold on;
plot (samp_points, output1(2,:), 'LineWidth', 1.5);
legend ("FHT", "DMS");
%xmin=0;
%xmax=2.5E-4;
%ymin=-4.8369;
%ymax=-4.83684127238243;
%axis([xmin xmax ymin ymax]); %x-axis limit is from 0 to 5, y-axis
   limit is from 0 to 50

title('Computation Times');
xlabel('Sampling Points');
ylabel('Time (sec)');
hold off

% for number distance 100 uses this
%mean_steady_state_hilbert= mean (output1(1, 90:100))
%mean_steady_state_dms= mean(output1(2, 90:100))

%for number of distances N, use ouptut(1, N-10: N) and, ouput(2, N
   -10: N)

mean_steady_state_hilbert= mean (output1(1, 5:10))
mean_steady_state_dcm= mean(output1(2, 5:10))
```

Listing A.3: hilbert dcm polt

Bibliography

[1] Yonas Muanenda. Recent advances in distributed acoustic sensing based on phase-sensitive optical time domain reflectometry. *Journal of Sensors*, 2018, 2018.

[2] Govind P Agrawal. *Fiber-optic communication systems*. John Wiley & Sons, 2012.

[3] Yonas Muanenda, Claudio J Oton, Stefano Faralli, and Fabrizio Di Pasquale. High performance distributed acoustic sensor using cyclic pulse coding in a direct detection coherent-otdr. In *Fifth Asia-Pacific Optical Sensors Conference*, volume 9655, pages 584–587. SPIE, 2015.

[4] Yonas Muanenda, Stefano Faralli, Claudio J Oton, Cheng Cheng, Minghong Yang, and Fabrizio Di Pasquale. Dynamic phase extraction in high-snr das based on uwfbgs without phase unwrapping using scalable homodyne demodulation in direct detection. *Optics express*, 27(8):10644–10658, 2019.

[5] Ali Masoudi and Trevor P Newson. High spatial resolution distributed optical fiber dynamic strain sensor with enhanced frequency and strain resolution. *Optics Letters*, 42(2):290–293, 2017.

[6] Yonas Muanenda, Stefano Faralli, Claudio J Oton, and Fabrizio Di Pasquale. Dynamic phase extraction in a modulated double-pulse ϕ-otdr sensor using a stable homodyne demodulation in direct detection. *Optics express*, 26(2): 687–701, 2018.

[7] Kjetil Johannessen, Brian Drakeley, and Mahmoud Farhadiroushan. Distributed acoustic sensing-a new way of listening to your well/reservoir. In *SPE Intelligent Energy International Conference and Exhibition*, pages SPE–149602. SPE, 2012.

[8] Jaehee Park and Henry F Taylor. Fiber optic intrusion sensor using coherent optical time domain reflectometer. *Japanese journal of applied physics*, 42 (6R):3481, 2003.

[9] Zuyuan He and Qingwen Liu. Optical fiber distributed acoustic sensors: A review. *Journal of Lightwave Technology*, 39(12):3671–3686, 2021.

[10] Yonas Muanenda, Stefano Faralli, Claudio J Oton, and Fabrizio Di Pasquale. Stable dynamic phase demodulation in a das based on double-pulse ϕ-otdr using homodyne demodulation and direct detection. In *Fiber Optic Sensors and Applications XV*, volume 10654, pages 106–115. SPIE, 2018.

[11] Zengguang Qin, Liang Chen, and Xiaoyi Bao. Continuous wavelet transform for non-stationary vibration detection with phase-otdr. *Optics express*, 20 (18):20459–20465, 2012.

[12] Sébastien Loranger, Mathieu Gagné, Victor Lambin-Iezzi, and Raman Kashyap. Rayleigh scatter based order of magnitude increase in distributed temperature and strain sensing by simple uv exposure of optical fibre. *Scientific reports*, 5(1):11177, 2015.

[13] Jun He, Lin Wang, Fang Li, and Yuliang Liu. An ameliorated phase generated carrier demodulation algorithm with low harmonic distortion and high stability. *Journal of Lightwave Technology*, 28(22):3258–3265, 2010.

[14] Lili Jin, Xingguang Li, and Meng Wu. Realization of fractional order integrator by rational function in the form of continued product. In *2015 IEEE International Conference on Mechatronics and Automation (ICMA)*, pages 1630–1635. IEEE, 2015.

[15] Zhou Sha, Hao Feng, and Zhoumo Zeng. Phase demodulation method in phase-sensitive otdr without coherent detection. *Optics Express*, 25(5):4831–4844, 2017.

[16] Zinan Wang, Li Zhang, Song Wang, Naitian Xue, Fei Peng, Mengqiu Fan, Wei Sun, Xianyang Qian, Jiarui Rao, and Yunjiang Rao. Coherent ϕ-otdr based on i/q demodulation and homodyne detection. *Optics express*, 24(2): 853–858, 2016.

[17] Yijie Sun, Xuan Li, Cun Ren, Hongzhong Xu, and Aimin Han. Distributed fiber optic sensing and data processing of axial loaded precast piles. *IEEE Access*, 8:169136–169145, 2020.

[18] Shih-Chu Huang and Hermann Lin. Modified phase-generated carrier demodulation compensated for the propagation delay of the fiber. *Applied optics*, 46(31):7594–7603, 2007.

[19] Fuyin Wang, Jiehui Xie, Zhengliang Hu, Shuidong Xiong, Hong Luo, and Yongming Hu. Interrogation of extrinsic fabry–pérot sensors using path-matched differential interferometry and phase generated carrier technique. *Journal of Lightwave Technology*, 33(12):2392–2397, 2014.

[20] Xiaojun Fang. Fiber-optic distributed sensing by a two-loop sagnac interferometer. *Optics letters*, 21(6):444–446, 1996.

[21] Yan Liu, Jun Jia, Pei-lin Tao, Zhong-wei Tan, Wen-hua Ren, Shui-sheng Jian, et al. Signal processing of sagnac fiber interferometer used as distributed sensor with wavelets. In *Asia Communications and Photonics Conference and Exhibition*, page 79900H. Optica Publishing Group, 2010.

[22] AE Alekseev, VS Vdovenko, BG Gorshkov, VT Potapov, and DE Simikin. A phase-sensitive optical time-domain reflectometer with dual-pulse phase modulated probe signal. *Laser Physics*, 24(11):115106, 2014.

[23] Anthony Dandridge, Alan B Tveten, and Thomas G Giallorenzi. Homodyne demodulation scheme for fiber optic sensors using phase generated carrier. *IEEE Transactions on microwave theory and techniques*, 30(10):1635–1641, 1982.

[24] Ailing Zhang and Shuai Zhang. High stability fiber-optics sensors with an improved pgc demodulation algorithm. *IEEE Sensors Journal*, 16(21):7681–7684, 2016.

[25] Jing-Feng Weng and Yu-Lung Lo. Novel rotation algorithm for phase unwrapping applications. *Optics Express*, 20(15):16838–16860, 2012.

[26] Zhongtao Cheng, Dong Liu, Yongying Yang, Tong Ling, Xiaoyu Chen, Lei Zhang, Jian Bai, Yibing Shen, Liang Miao, and Wei Huang. Practical phase unwrapping of interferometric fringes based on unscented kalman filter technique. *Optics express*, 23(25):32337–32349, 2015.

[27] Abdulnasir Hossen. A new fast approximate hilbert transform with different applications. *IIUM Engineering Journal*, 2(2), 2001.

[28] Alexander D Poularikas. *Handbook of formulas and tables for signal processing*. CRC press, 2018.

[29] RJ Henery. Hilbert transforms using fast fourier transforms. *Journal of Physics A: Mathematical and General*, 17(18):3415, 1984.

[30] John Essick. *Hands-on introduction to LabVIEW for scientists and engineers*. Oxford University Press, USA, 2013.

[31] Cor J Kalkman. Labview: A software system for data acquisition, data analysis, and instrument control. *Journal of clinical monitoring*, 11:51–58, 1995.

[32] Hsi-Ping Liu and Dan D Kosloff. Numerical evaluation of the hilbert transform by the fast fourier transform (fft) technique. *Geophysical Journal International*, 67(3):791–799, 1981.